ISSN 0021-3640, JETP Letters, 2017, Vol. 105, No. 7, pp. 453–457. © Pleiades Publishing, Inc., 2017.
Original Russian Text © O.A. Kosmachev, Yu.A. Fridman, B.A. Ivanov, 2017, published in Pis'ma v Zhurnal Eksperimental'noi i Teoreticheskoi Fiziki, 2017, Vol. 105, No. 7, pp. 444–448.

CONDENSED MATTER

Phase States of a Magnetic Material with the Spin $S = 2$ and the Isotropic Exchange Interaction

O. A. Kosmachev[a], Yu. A. Fridman[a], and B. A. Ivanov[b, *]

[a] *Vernadsky Crimean Federal University, Simferopol, 295007 Russia*
[b] *Institute of Magnetism, National Academy of Sciences of Ukraine, Kyiv, 03142 Ukraine*
** e-mail: bor.a.ivanov@gmail.com*

Received January 24, 2017; in final form, March 9, 2017

A phase diagram of a magnetic material with the spin $S = 2$ is obtained including all allowed spin invariants for the isotropic exchange interaction at an arbitrary relation between exchange constants. New phases with two-sublattice structure and biaxial symmetry at a site are found.

DOI: 10.1134/S0021364017070086

1. Interest in study of new phase states of spin systems of magnetic materials has grown for the last three decades [1–7]. Isotropic magnetic materials with the spin $S > 1/2$ can exhibit not only phases with a magnetic order, i.e., with a nonzero average value of the spin at the site $\langle \mathbf{S} \rangle$, but also phases with $\langle \mathbf{S} \rangle = 0$, where the spontaneous breaking of rotational symmetry is due to the average values of spin multipoles. Such a state called spin nematic was first found for magnetic materials with the spin $S = 1$ [1–3]. The geometric image of this phase is a quadrupole ellipsoid representing the tensor $S_{ij} = \langle S_i S_j + S_j S_i \rangle /2$, which is an ellipsoid of revolution of the ground state, and the symmetry of the state at the site is C_∞. For this system, an orthogonal nematic phase with perpendicular principal axes of quadrupole ellipsoids was also found [5]. For higher spins $S > 1$, nematic phases demonstrate qualitatively novel properties. Phases with $\langle \mathbf{S} \rangle = 0$ were found for the spin $S = 3/2$; for these phases, the time reversal symmetry is broken because of the three-spin averages (two-dimensional pseudospin vector $\boldsymbol{\sigma}$) [3, 6] and antinematic phases with antiparallel $\boldsymbol{\sigma}$ vectors in the sublattice [6]. Two different types of nematic states of the system with the spin $S = 2$ [7] and fractional vortices in these phases [8] were studied.

Nematic states appear for models including all higher exchange invariants of the form $(\mathbf{S}_1\mathbf{S}_2)^n$ with $n \le 2S$. In many magnetic materials, the contribution of higher exchanges is much smaller than the Heisenberg contribution, but nematic phases of spin systems with $S \ge 1$ are important for studying states of ultracold atomic gases in optical traps [9], for which higher exchange integrals are not small [7, 10]. Condensates of ^{87}Rb and ^{23}Na atoms with the spin $S = 2$ are experimentally implemented [11].

In this work, we study phase states and their stability for a model of an isotropic magnetic material with the spin $S = 2$ including the interaction between nearest neighbors at low temperatures in the mean field approximation. We find new phases with a two-sublattice structure and plot the phase diagram at an arbitrary relation between the parameters of the Hamiltonian.

2. The Hamiltonian of the isotropic magnetic material with the spin $S = 2$ including the complete set of spin invariants has the form

$$\widehat{H} = -\frac{1}{2}\sum_{\mathbf{n},\mathbf{n}'}\Big[J(\mathbf{S}_\mathbf{n}\mathbf{S}_{\mathbf{n}'}) + K(\mathbf{S}_\mathbf{n}\mathbf{S}_{\mathbf{n}'})^2 + D(\mathbf{S}_\mathbf{n}\mathbf{S}_{\mathbf{n}'})^3 + F(\mathbf{S}_\mathbf{n}\mathbf{S}_{\mathbf{n}'})^4\Big], \qquad (1)$$

where summation is performed over all pairs of nearest neighbors on the lattice allowing the decomposition into two sublattices with translation vectors $\mathbf{n}$ and $\mathbf{n}'$ and J, K, D, and F are the exchange integrals.

The state vector of the system can be represented in the form of the direct product of state vectors of the spin operator $\mathbf{S}_\mathbf{n}$ with $S = 2$ at each site $\mathbf{n}$. The state vector at a given site can be written in the form of a superposition of five vectors $|m\rangle$ with a given spin projection m on the quantization axis (z axis), $m = \pm 2, \pm 1, 0$, $|\psi\rangle = \sum_m C_m |m\rangle$, where the coefficients C_m belong to the complex projective space CP^4. At low temperatures (in the limit $T \to 0$), the energy of the system in the molecular field approximation coincides with the average value of the Hamiltonian over the state vector, $W[C_{m,\mathbf{n}}] = \langle\widehat{H}\rangle$.

For the simplest single-sublattice phases, the states of spins at each site are identical and the energy $W = W(C_m)$ depends on eight real parameters. In view of the isotropy of the system, the number of independent parameters can be reduced. We assume that the average spin, if it is nonzero, is parallel to the z axis. Then, $\langle S_x\rangle = \langle S_y\rangle = 0$, only the superpositions of $|m\rangle$ with m values differing by no less than 2 can be written, and the tensor S_{ij} can be chosen diagonal. Under these conditions, one can consider only two forms of the trial state vector at the site, $|\psi_1\rangle$ or $|\psi_2\rangle$:

$$|\psi_1\rangle = \cos\theta|2\rangle + \sin\theta|-1\rangle, \quad (2)$$

$$|\psi_2\rangle = \cos\beta(\cos\varphi|2\rangle + \sin\varphi|-2\rangle) + \sin\beta|0\rangle. \quad (3)$$

Further, it is easy to express the free energy of the system at zero temperature for each of the functions $|\psi_{1,2}\rangle$ in terms of the parameters θ or φ, β, respectively. The stability of the found phases will be discussed below.

We begin with the vector $|\psi_1\rangle$, for which the energy (per spin) is given by the expression

$$W_1 = -\frac{1}{4}(\tilde{J} + 3\tilde{K})(1 - 3\cos^2\theta)^2, \quad (4)$$

where $\tilde{J} = 2J - K + 41D - 79F$ and $\tilde{K} = K - 5D + 43F$.

It is easily seen that the minimum at $\tilde{J} + 3\tilde{K} > 0$ corresponds to a ferromagnetic state in which $\theta = 0$ and $|\psi\rangle = |\psi_{FM}\rangle = |2\rangle$; i.e., the average value of the spin at the site is maximal, $\langle S_z\rangle = 2$. The second state with Eq. (2) appears at $\tilde{J} + 3\tilde{K} < 0$ and corresponds to $\cos\theta = 1/\sqrt{3}$ and the state vector

$$|\psi\rangle = |\psi_{\mathrm{TN}}\rangle = (|2\rangle + \sqrt{2}|-1\rangle)/\sqrt{3}. \quad (5)$$

Such a state was found in the model of the Bose gas of atoms with the spin $S = 2$ and contact interaction [7] with the use of the Majorana representation (the spin state S is determined by $2S$ points on the unit sphere, see [12]). These four points for the state given by Eq. (5) coincide with the vertices of a tetrahedron [7]; therefore, it is reasonable to call this state tetrahedral nematic, for which $\langle\mathbf{S}\rangle = 0$, and the quadrupole ellipsoid is degenerate into a sphere, $\langle S_x^2\rangle = \langle S_y^2\rangle = \langle S_z^2\rangle = 2$. The spontaneous breaking of symmetry is determined by averages, which are cubic in the components of the spin operator and are not invariant with respect to time reversal $t \to -t$. For the particular form (5), only $\langle (S^+)^3 + (S^-)^3\rangle = 8\sqrt{2}$ and $\langle S_z^3\rangle = 2$ are nonzero. For the visual representation of their geometric properties, we note that $\langle (S_x\cos\chi + S_y\sin\chi)^3\rangle = \sqrt{2}\cos 3\chi$, which is invariant with respect to rotations about the z axis by an angle of $2\pi/3$. This indicates the existence of the third-order axis C_3 coinciding with the z axis. The same properties occur for three directions that make an angle of $2\arctan\sqrt{2} \simeq 109.5°$ with the z axis and have the polar angles of $\pi/3, \pi, 5\pi/3$. The z axis and these three axes are oriented as the axes of the C_3 tetrahedron with one of the vertices at a positive z value.

The energy for the second trial function $|\psi_2\rangle$ given by Eq. (3) is described by the formula

$$W_2 = \frac{3}{2}\tilde{K}(1 - \sin 2\varphi)\sin^2 2\beta - \tilde{J}\cos^2 2\varphi\cos^4\beta - 3\tilde{K}. \quad (6)$$

The minimization of Eq. (6) gives not only ferromagnetic and tetrahedral nematic states (when $\varphi = 0$, $\beta = 0$ and $\varphi = -\pi/4$, $\beta = \pi/4$) but also a new spin nematic state at $\varphi = \pi/4$ with zero spin $\langle\mathbf{S}\rangle = 0$, for which

$$|\psi_{\mathrm{SN}}\rangle = \frac{1}{\sqrt{2}}\cos\beta(|2\rangle + |-2\rangle) + \sin\beta|0\rangle, \quad (7)$$

and the energy given by Eq. (6) is independent of β. The geometric image of the spin nematic state in the spin space at $\beta \neq 0, \pi/2$ is a biaxial ellipsoid

$$\langle S_z^2\rangle = 4\cos^2\beta, \quad \langle S_{x,y}^2\rangle = (\sqrt{3}\sin\beta \pm \cos\beta)^2. \quad (8)$$

We recall that quadrupole ellipsoids for nematic states of magnetic materials with $S = 1$ and $S = 3/2$ are uniaxial (symmetry C_∞), which in the case of Eq. (8) occurs only at $\beta = 0$ and $\pi/2$. The total symmetry C_∞ is present only at $\beta = \pi/2$ when $\langle S_z^2\rangle = 0$ and $\langle S_x^2\rangle = \langle S_y^2\rangle = 3$, and the ellipsoid is degenerate into a flat disk. The quadrupole ellipsoid at $\beta = 0$ is also uniaxial, $\langle S_z^2\rangle = 4$, $\langle S_x^2\rangle = \langle S_y^2\rangle = 1$, but the symmetry of the state is reduced owing to fourth order averages, $2\langle (S_x\cos\chi + S_y\sin\chi)^4\rangle = 3\cos 4\chi + 5$; i.e., the single-site state at $\beta = 0$ is characterized by the C_4 symmetry axis [7]. The authors of [13] showed that the inclusion of thermal fluctuations results in the choice of only one of two values, $\beta = 0$ or $\beta = \pi/2$ (it will be shown below that the state with $\beta = \pi/4$ is also possible).

States of the magnetic material in the model given by Eq. (1) can include phases with different spin states in two sublattices. The existence of an antiferromagnetic state is obvious. The unitary transformation $U(\varphi) = \prod_{n'}\exp(i\pi S_{\mathbf{n}',x})$, i.e., the rotation of the spins of the second sublattice by the angle $\varphi = \pi$ about the x axis, reduces the problem to the study of a homogeneous state for the Hamiltonian given by Eq. (1). Similar to magnetic materials with $S = 1$ and 3/2, the antiferromagnetic state is characterized by the saturated spin values $|\mathbf{S}_{\mathbf{n},\mathbf{n}'}| = 2$ and by the antiparallel orientation of spins of sublattices.

To analyze the stability of the phases described above with respect to arbitrary small perturbations, we find the spectrum of all branches of elementary excitations (magnons) $\varepsilon_\alpha(\mathbf{k})$. For a magnetic material with the spin $S = 2$, there are four such branches, $\alpha = 1$–4 specifies the mode number, and $\mathbf{k}$ is the wave vector belonging to the Brillouin zone. The presence of instabilities at $\mathbf{k}$ values that are not low not only indicate transitions to multisublattice phases but also allow understanding their sublattice structure. Magnon spectra were obtained by the Green's function method for the Hubbard operators [14, 15]. The analysis is almost the same as that for the magnetic material with the spin $S = 3/2$ [16]; for this reason, we omit the details of the calculation. The representation of the results in terms of four exchange constants is clearer for the following combinations of the variables $\lambda_1 = 2J - K + 41D - 70F$, $\lambda_2 = 3(D - 5F)$, $\lambda_3 = K - 2D + 28F$, and $\lambda_4 = 9F$ for the real projective space

$$x = \lambda_1/\lambda_4, \quad y = \lambda_2/\lambda_4, \quad z = \lambda_3/\lambda_4, \tag{9}$$

considering its cross sections at a fixed z value.

The simplest spectra are characteristic of the tetrahedral nematic phase because three branches for it are degenerate and have a linear dispersion law at $\mathbf{k} \to 0$, in agreement with the general result on the number of gapless magnon branches [17] in the presence of a high (tetrahedral) symmetry of the state at the site. The indicated three branches correspond to the turns of axes of tetrahedra and the corresponding oscillations of the average spin. Instability associated with these branches determines transitions to states with a nonzero spin. Such an instability with respect to perturbations with small values $\mathbf{k} \to 0$ or with $\mathbf{k} \to \mathbf{k}_B$, where $\mathbf{k}_B$ corresponds to the edge of the Brillouin zone, occurs at $x - 3y + 3z > 1$ or $x + 3y + 3z < -1$, respectively. The fourth branch (with a finite energy gap) is determined by oscillations of multipole moments at $\langle \mathbf{S}(t) \rangle = 0$. Under the conditions $y < z$ or $y < -z$ for perturbations with $\mathbf{k} \to 0$ or with $\mathbf{k} \to \mathbf{k}_B$, respectively, it describes the instability with respect to a transition to other nematic states.

In the ferromagnetic phase, one of the four excitation branches is gapless and corresponds to the precession of the spin. The stability of the ferromagnetic phase is determined by activation branches. The ferromagnetic phase loses its stability with respect to long-wavelength perturbations ($\mathbf{k} \to 0$) at $x - 3y + 3z < 1$ and at $x < 1$. Thus, the region of stability of the tetrahedral nematic and ferromagnetic phases can touch each other at $x - 3y + 3z = 1$ and $x = 1$. Instability with respect to perturbations with $\mathbf{k} \to \mathbf{k}_B$ occurs at $x + 3y + 9z < 1$, which indicates a transition to a two-sublattice phase.

For the antiferromagnetic phase, states of spins in different sublattices are energetically equivalent, and it is reasonable to consider magnons in the expanded band scheme. For all four branches of the spectrum, the energies are determined by the relation $\epsilon_\alpha^2(\mathbf{k}) = A_\alpha^2 - B_\alpha^2 C^2(\mathbf{k})$, where $ZC(\mathbf{k}) = \sum_{\mathbf{b}} \exp(i\mathbf{b}\cdot\mathbf{k})$, $\mathbf{b}$ is the set of Z vectors of nearest neighbors, $C(\mathbf{k}) \to 1$ at $\mathbf{k} \to 0$, and $C(\mathbf{k}) \to -1$ at $\mathbf{k} \to \mathbf{k}_B$. One of these branches is Goldstone and $A_G = B_G = 2(5K + 179F - J - 34D)$ and $\epsilon_G \to c|\mathbf{k}|$ at $\mathbf{k} \to 0$ for it. Since $c \propto A_G$, the antiferromagnetic phase is unstable at $x + 3y - 9z > -1$. The analysis also indicates the presence of instabilities of the antiferromagnetic phase at $x - 3y - 3z > -1$ and $x > -1$.

Thus, the picture of transitions is more complex than that for the magnetic material with the spin $S = 3/2$, where the regions of stability of phases were determined by signs of only two combinations of the parameters, Λ_1 and Λ_2 (see [6]). The analysis is difficult also because the form of magnon spectra of the spin nematic phase depends on the parameter β (see below). However, the picture of phase states is the simplest for $z = 0$ and it is appropriate to begin with the analysis of this case.

The nematic phase does not appear at $z = 0$ (more precisely, the conditions of its stability at any β value are satisfied only on the line segment $z = 0$, $y = 0$, $-1 < x < 1$). Both the ferromagnetic and antiferromagnetic phases become unstable on the straight lines $x \pm 3y = 1$ and $x \pm 3y = -1$, whereas the tetrahedral nematic phase is stable at $3y + x + 1 > 0$, $3y - x + 1 > 0$, and $y > 0$ (Fig. 1). The regions of stability of these three phases on the (x, y) plane are bounded from below by lines on which instability with respect to perturbations with $\mathbf{k} \to \mathbf{k}_B$ occurs; i.e., a certain two-sublattice phase should appear in the remaining part of the plane. The analysis shows that this two-sublattice phase has a tetrahedral symmetry ($\langle \mathbf{S} \rangle = 0$ and $S_{ij} = 2\delta_{ij}$) at each site, and the states $|\psi_\mathbf{n}\rangle$ and $|\psi_{\mathbf{n}'}\rangle$ in each of the sublattices have the form of orthogonal vectors

$$\sqrt{3}|\psi_\mathbf{n}\rangle = |2\rangle + \sqrt{2}|-1\rangle, \quad \sqrt{3}|\psi_{\mathbf{n}'}\rangle = |-2\rangle - \sqrt{2}|1\rangle. \tag{10}$$

The nontrivial averages of the spin components for the first and second sublattices have opposite signs, $\langle (S_1^z)^3 \rangle = 2$ and $\langle (S_2^z)^3 \rangle = -2$,

$$\langle (S_{1,2}^x \cos\chi + S_{1,2}^y \sin\chi)^3 \rangle = \pm\sqrt{2}\cos 3\chi,$$

and it is reasonable to call this state the tetrahedral antinematic phase. The geometric images of states in

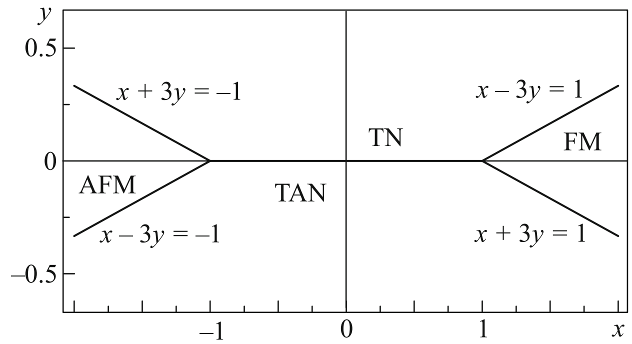

Fig. 1. Regions of existence of various phases on the $z = 0$ plane in the space of parameters of the problem specified by Eq. (9). Here and in Fig. 2: FM is the ferromagnetic phase, AFM is the antiferromagnetic phase, TN is the tetrahedral nematic, and TAN is the tetrahedral antinematic.

each of the sublattices for it are tetrahedra with opposite directions of vertices, which are turned with respect to each other about the z axis by an angle of $\pi/3$.

The tetrahedral antinematic phase, as well as the tetrahedral nematic phase, possesses three degenerate gapless magnon branches and the fourth branch has finite activation. The conditions of stability of the tetrahedral antinematic phase include the inequalities $x + 3y - 3z < 1$ and $x - 3y - 3z > -1$. Furthermore, instabilities with respect to perturbations with $\mathbf{k} \to 0$ or with $\mathbf{k} \to \mathbf{k}_B$ occur under the conditions $y < z$ or $y > -z$, respectively. These two conditions are opposite to the conditions for the tetrahedral nematic phase, and the regions of stability of the tetrahedral nematic and tetrahedral antinematic phases at $z = 0$ touch each other on the line segment $y = 0$, $-1 < x < 1$. Thus, the four phases described above completely determine all states of the system at $z = 0$. Transitions between phases, as for the cases $S = 1$ and $3/2$, are first order degenerate phase transitions.

The behavior of the system is significantly different for the cases $z > 0$ and $z < 0$. We consider the behavior of the spin nematic phase, whose energy is independent of the parameter β, near the phase transition lines. At $y = z$ or $y = -z$, these transitions occur from the spin nematic phase to the tetrahedral nematic or tetrahedral antinematic phase, respectively, whereas at $x = 1$ or $x = -1$, the spin nematic phase transits to the ferromagnetic or antiferromagnetic phase, respectively. In contrast to the energy, the character of magnon spectra depends significantly on β. In particular, the spin nematic phase with the symmetry C_∞ ($\beta = \pi/2$) includes pairwise degenerate modes: two activation modes and two modes with zero gap and a linear dispersion law. For $\beta \neq \pi/2$, 0, there are three modes with a linear dispersion law and different velocities, but the velocities of two of them coincide at $\beta = 0$ when the system has a higher symmetry C_4.

In the spin nematic phase, modes with $\beta = \pi/2$ are softened near transition lines to the ferromagnetic or antiferromagnetic phase and modes with $\beta = 0$ are softened near transition lines to the tetrahedral nematic or tetrahedral antinematic phase. These β values should be expected in the spin nematic phase. This corresponds to the result reported in [13], according to which a fixed β value is determined by thermal corrections to the free energy of the spin nematic phase (the so-called order-by-disorder mechanism). This correspondence is clear: the softer mode makes a more significant contribution to the free energy. The transition lines between spin nematic phases with $\beta = \pi/2$ and $\beta = 0$ are determined by the conditions $x \pm 1 = \pm 9z(y - z)$ and $x \pm 1 = \pm 9z(y + z)$ (Fig. 2).

Thus, the spin nematic phase exists only at $z > 0$ inside the rectangle $-z < y < z$ and $|x| < 1$. On all these lines, as well as on (ferromagnetic $\rightleftarrows$ tetrahedral nematic) and (antiferromagnetic $\rightleftarrows$ tetrahedral antinematic) transition lines, first order degenerate phase transitions occur. However, a finite region of coexistence of phases with different sublattice structures exists at $z > 0$ (see Fig. 2). The energies of two phases become equal to each other on the first order transition lines $x + 3y - 3z = -1$ and $x + 3y + 3z = 1$; these lines and lines of stability of coexisting phases converge at the points ($x = -1$, $y = z$) or ($x = 1$, $y = -z$).

The nematic phase of the form (7) does not exist at $z < 0$ and one can expect the appearance of a two-sublattice orthogonal nematic phase [5]. The structure of the orthogonal nematic phase is determined by states (3) with the values $\varphi_{1,2}$ and $\beta_{1,2}$ in sublattices. The analysis shows that the φ parameters in sublattices coincide with each other, whereas the β_1 and β_2 values differ by $\pi/2$. The inclusion of thermal corrections separates the values $\beta = \pi/4$ and $\beta = -\pi/4$. In this case, quadrupole ellipsoids are biaxial with the principal axes $\mathbf{e}_1$, $\mathbf{e}_2$, and $\mathbf{e}_3$ and values $\langle S_1^2 \rangle = 2 + \sqrt{3}$, $\langle S_2^2 \rangle = 2$, and $\langle S_3^2 \rangle = 2 - \sqrt{3}$. The "intermediate" $\mathbf{e}_2$ axes for different sublattices are collinear and the axes with the maximum and minimum $\langle S_i^2 \rangle$ values are perpendicular to each other. The magnon spectrum in this phase has four modes, three of which are gapless. According to the analysis of spectra of elementary excitations, the region of existence of the orthogonal nematic phase is determined by the inequalities $z < y < -z$ and $3y + 3z - 1 < x < 3y - 3z + 1$. In this case, two regions (marked by LS in Fig. 2b) remain on the (x, y) plane, where two-sublattice phases exist with a symmetry lower than the symmetry of phases adjacent to them (antiferromagnetic and tetrahedral nematic or ferromagnetic and tetrahedral antinematic for the left or right LS region, respectively). For LS phases, both (unsaturated) spins of the sublattices and correlation

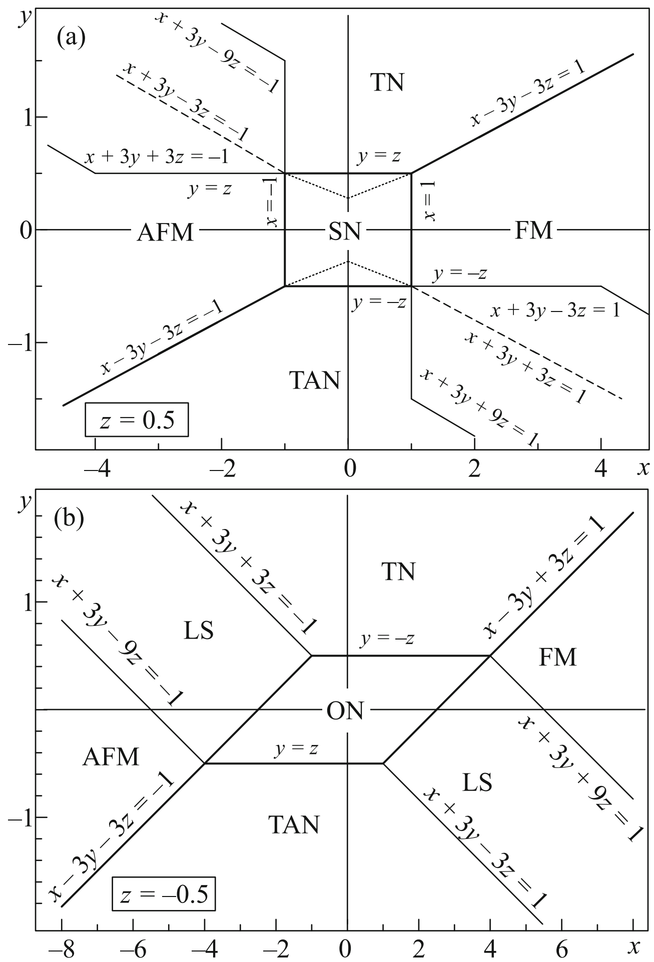

Fig. 2. Regions of existence of various phases on the z = const ≠ 0 plane in the space of the variables x, y, z at z = (a) 0.5 and (b) −0.5. Here, SN is the spin nematic, ON is the orthogonal nematic, LS stands for phases with the lowest symmetry, and the other notation is the same as in Fig. 1. The dashed lines mark standard first order phase transitions, thin solid lines are the lines of loss of stability of phases, and dotted lines are the boundaries of the spin nematic phases with $\beta = 0$ and $\beta = \pi/2$.

functions $\left\langle (S_x \cos\chi + S_y \sin\chi)^3 \right\rangle = C\cos 3\chi$, $|C| < \sqrt{2}$, are nonzero; of four C_3 axes characteristic of the tetrahedral nematic and tetrahedral antinematic phases, only one axis parallel to the z axis "survives."

3. To summarize, we have completely analyzed the phases of a magnetic material with the spin $S = 2$ and the general form of isotropic interaction (1). The appearance of nondegenerate phase transitions between phases has been revealed for the first time: depending on the sign of the parameter z, either the first order phase transition with a finite region of coexistence of phases or two second order phase transitions through a phase with a low symmetry occur. In contrast to systems with $S = 1$ and 3/2 with the symmetry C_∞ at the site, in systems with $S = 2$, we have found phases for which the symmetry at the site is discrete: an orthogonal nematic phase with a biaxial symmetry, as well as tetrahedral nematic and tetrahedral antinematic phases with a tetrahedral symmetry at the site. Because of the nontrivial properties of the order parameter of these phases, three Goldstone branches of elementary excitations [17], as well as features of topological defects, appear. The homotopic group π_1 for the found phases is noncommutative, and non-Abelian topological defects known for standard biaxial nematics exist [18–20]. The possibility of experimental excitation of nontrivial topological defects (fractional vortices) for systems with $S = 2$ was discussed in [8].

We are grateful to G.E. Volovik for stimulating discussions of the topological properties of the found phases. This work was supported in part by the Russian Foundation for Basic Research (project nos. 16-02-00069 (for Yu.A.F. and O.A.K.) and 16-42-910441 (for O.A.K.)).

REFERENCES

1. A. F. Andreev and I. A. Grishchuk, Sov. Phys. JETP **60**, 267 (1984).
2. N. Papanikolaou, Nucl. Phys. B **305**, 367 (1988).
3. A. V. Chubukov, J. Phys.: Condens. Matter **2**, 1593 (1990).
4. V. I. Butrim, B. A. Ivanov, and A. S. Kuznetsov, JETP Lett. **92**, 151 (2010).
5. Yu. A. Fridman, O. A. Kosmachev, and Ph. N. Klevets, J. Magn. Magn. Mater. **325**, 125 (2013).
6. Yu. A. Fridman, O. A. Kosmachev, A. K. Kolezhuk, and B. A. Ivanov, Phys. Rev. Lett. **106**, 097202 (2011).
7. R. Barnett, A. M. Turner, and E. Demler, Phys. Rev. Lett. **97**, 180412 (2006).
8. J. A. M. Huhtamäki, T. P. Simula, M. Kobayashi, and K. Machida, Phys. Rev. A **80**, 051601(R) (2009).
9. O. Morsch and M. Oberthaler, Rev. Mod. Phys. **78**, 179 (2006).
10. F. Zhou and M. Snoek, Ann. Phys. (N.Y.) **308**, 692 (2003).
11. H. Schmaljohann, M. Erhard, J. Kronjäger, M. Kottke, S. van Staa, L. Cacciapuoti, J. J. Arlt, K. Bongs, and K. Sengstock, Phys. Rev. Lett. **92**, 040402 (2004).
12. H. Bacry, J. Math. Phys. (N.Y.) **15**, 1686 (1974).
13. A. M. Turner, R. Barnett, E. Demler, and A. Vishwanath, Phys. Rev. Lett. **98**, 190404 (2007).
14. R. O. Zaitsev, Sov. Phys. JETP **41**, 100 (1975).
15. Yu. A. Fridman, O. A. Kosmachev, and Ph. N. Klevets, J. Magn. Magn. Mater. **320**, 435 (2008).
16. O. A. Kosmachev, Yu. A. Fridman, E. G. Galkina, and B. A. Ivanov, J. Exp. Theor. Phys. **120**, 281 (2015).
17. A. F. Andreev and V. I. Marchenko, Sov. Phys. Usp. **23**, 21 (1980).
18. G. E. Volovik and V. P. Mineev, Sov. Phys. JETP **45**, 1185 (1977).
19. V. Poenaru and G. Toulouse, J. Phys. (Paris) **8**, 887 (1977).
20. N. D. Mermin, Rev. Mod. Phys. **51**, 591 (1979).

Translated by R. Tyapaev